Experimental and Theoretical Analysis of Electropolymerized PMeT Thin Films

S. VELUMANI,[1] J. A. ASCENCIO,[2] G. CANIZAL,[3] P. J. SEBASTIÁN,[4] J. GARCÍA-SERRANO,[5] U. PAL[6]

[1]Departamento de Física, Instituto Tecnológico y de Estudios Superiores de Monterrey. Monterrey, N.L. Mexico

[2]Programa de Ingeniería Molecular. Instituto Mexicano del Petróleo, Eje Central Lázaro Cárdenas No. 152, C. P. 07730 Mexico D.F., Mexico

[3]Centro de Educación Continúa y a Distancia (Unidad Allende), Instituto Politécnico Nacional, Allende No. 38, Centro, México D.F. 06010, Mexico

[4]Centro de Investigación en Energía, UNAM, Temixco, Morelos 62580, Mexico

[5]Centro de Investigaciones en Materiales y Metalurgia, Universidad Autónoma de Estado de Hidalgo, Carr. Pachuca-Tulancingo, Km. 4.5, Pachuca, Hgo. C.P. 42184, Mexico

[6]Instituto de Física, Universidad Autónoma de Puebla, Puebla, C.P. 72570, Mexico

Received 28 February 2005; revised 14 July 2005; accepted 1 August 2005
DOI: 10.1002/polb.20602
Published online in Wiley InterScience (www.interscience.wiley.com).

ABSTRACT: It is reported that the physical analysis of poly(3-methylthophene) (PMeT) thin films were doped with BF_4^- anions, which were deposited on tin oxide-coated glass and stainless steel substrates using electropolymerization technique. The atomistic and electronic structures were evaluated to understand the main principles for the pure and doped PMeT polymers that give the photonic and conductivity properties for this kind of materials. It is found that galvanostatic method is more suitable for the electropolymerization of PMeT on conducting glass or flexible metal surfaces. The films were characterized using SEM, AFM, XRD, FTIR, Raman, and UV–vis absorption techniques. Raman and FTIR spectra of the samples revealed no signal related to the Li or the anion BF_4^- dopant, indicating that the optimum dopant concentration was well below the threshold value. Apart from the dopant influence, which is a well understood phenomenon, an attempt has been made to explain the influence of the lithium in the polymer matrix. The Li^+ ions incorporated into the PMeT films form highly confined conjugational defects, neither dynamically nor electronically coupled with the host lattice. Using density function theory calculations, we could determine the optimum geometrical configurations of the cis and trans polymers and their corresponding electronic structure modification because of the presence of Li^+ atoms controlling the electronic band gaps. © 2005 Wiley Periodicals, Inc. J Polym Sci Part B: Polym Phys 43: 3058–3068, 2005

Keywords: conductive polymers; PMeT; polymer characterization; structure determination; theoretical analysis

INTRODUCTION

The search for low cost solar energy conversion systems has formed the base for introduction of several new organic–inorganic hybrid or junction

Correspondence to: J. A. Ascencio (E-mail: ascencio@imp.mx)

Journal of Polymer Science: Part B: Polymer Physics, Vol. 43, 3058–3068 (2005)

structures in the list of solar energy materials in recent years. Since the first report made by Horowitz and Garnier[1] on GaAs-PT (PT, polythiophene) heterojunctions, several workers have demonstrated the possibility of using polymers as the efficient solar absorber. As the part of the heterojunction, the polymer films control the energy conversion yield of a photovoltaic device. Apart from the GaAs-PT heterostructures,[1] Frank et al.[2] and Chartier et al.[3–5] have reported the fabrication of CdS-PMeT (PMeT, poly(3-methylthophene)) Schottky junctions with 1.3% energy conversion efficiency. By creating the localized energy levels in the band gap of chemically deposited CdS films, Chartier et al.[3] could improve the energy conversion efficiency of Schottky-type photovoltaic junctions up to 2.7%. On the other hand, modification of both CdS band gap and the conductivity of PMeT caused an improvement of the energy conversion efficiency up to 4%.[5] Therefore, for improving the energy conversion efficiency of such organic–inorganic structures, the modifications of both the components are very important. As the polymers in Schottky-type junctions behave like metal, the control of their electrical conductivity is of immense importance for their use in solar cells. In most of the works, the polymer films were deposited by electropolymerization on semiconductor film surfaces. Though the polymer films were doped to improve their electrical conductivity, there are not many reports on the characterization of basic properties of such polymer films, which would be very much useful for their applications in solar cells.

PT and its derivatives represent a particularly interesting family of polymers. In contrast to many other conductive polymers, they are relatively stable against oxygen and moisture in both their doped and undoped states. The PTs also posses a nondegenerate ground state. One of the most important factors for the use of organic systems in photoconductive or photovoltaic devices is the electronic structure modifications with the inclusion of certain elements, where the knowledge of the orbital distributions behavior of the molecular systems in presence of doping elements as well as the presence of the salt containing the dopant becomes quite important for designing a device. In fact, the self-configuration of the polymer is another variable in the band gap generation and worth a further detailed analysis. The use of experimental and theoretical methods in conjunction opens up the perspectives to develop materials and devices based on the electronic structure modifications both in crystals and molecular systems.[6–8] Particularly, the quantum mechanical calculation method helps to determine the lowest energy configurations and to know how this involves a particular orbital distribution making favorable for charge conduction.

In the present work, we report the synthesis of PMeT thin films on conducting glass and metal substrates by electropolymerization with lithium tetrafluoroborate to accommodate BF_4^- as anionic dopant and characterized by X-ray diffraction (XRD), scanning electron microscope (SEM), AFM, cyclic-voltametry, and optical spectroscopy techniques. As the mechanism of charge generation and the effect of anions in the π–π^* band gap are well reported,[9,10] we performed theoretical calculations using density function theory (DFT) to study the intercalation mechanism of Li atoms with the polymer matrix. Apart from the optimization of the geometry, electronic parameters such as charge distribution, frontier orbital distributions, and electrostatic potential were determined to understand how the Li atoms modify the electronic structure of the polymer to tailor its optical and electrical properties.

EXPERIMENTAL AND THEORETICAL TECHNIQUES

Electropolymerization is carried out in a single compartment electrochemical cell by adopting a standard three electrode configuration consisting of Ag/AgCl as reference electrode, graphite as counter electrode, and the substrate, either stainless steel or conducting glass, as working electrode. The electrolyte consists of 3-methyl thiophene (0.1 M) monomer in the propylene carbonate solvent along with either lithium tetrafluoroborate (0.1 M) or lithium perchlorate (0.1 M) as dopant solution. The solutions were deoxygenated for 30 min with nitrogen gas flow and maintained under nitrogen atmosphere throughout the deposition process. Tin oxide (TO) films were spray deposited on Pyrex glass slides (transmittance about 75% at 700 nm) and used for electropolymerization of PMeT films. Electropolymerization of PMeT films was done on TO glass slides of 2 cm^2 area and stainless

steel foils (0.05 cm thick, ASI 301, Good Fellow) as substrates.

Electropolymerization was carried out at different constant potentials (E) between 0.5 and 2.0 V. The grown films were not uniform for all the potentials and controlling the deposition process was difficult. In most of the cases, the oligomeric species fell down from both SS- and TO-coated glass substrates. Therefore, we tried to use galvanostatic method for the electropolymerization of the PMeT. Electropolymerization of PMeT at different constant current densities in between 3.0 and 1 mA/cm^2 gave well uniform, homogeneous films on both the substrates. The evolution of the PMeT film formation was monitored so as to follow the deposition and electrochemical profiles, which allows a better control over the deposition parameters and to improve the deposition process.

Thickness of the PMeT films was measured using a Tenchor Alphastep 100 surface profilometer. CuK_α radiation of a Rigaku RINT 2100 diffractometer was used for recording the XRD traces of the films. A Shimadzu UV-VIS-NIR (model 365) double beam spectrophotometer was used for recording the transmittance and reflectance spectra of the films between 440 and 2500 nm wavelengths. For the analysis of surface morphology of the films, a JEOL JSM 6400 SEM and a DI SPM Nanoscope4 in contact mode were used. The conductivity of the films was estimated using four probe technique. Conductivity type of the samples was determined using hot probe technique. A Nicolet Magna 750 FTIR spectrometer was used to record the IR absorption spectra in diffuse mode. Raman spectra were recorded on a Raman PerkinElmer system 2000 spectrophotometer.

A molecular model is proposed for the monomer in a small polymer configuration, which is geometry-optimized to identify the minimum energy structure to explain the bond formations as revealed in the experimental data. From the geometry optimization, an improvement for the atomistic and electronic structures was made using the DMol3 program based on the density function theory (DFT).[11,12] To have optimum results, we used the local density approximation and the Perdew-Wang functional with an electronic integration accuracy based on a self consistent field tolerance of 1×10^{-6} Ha. This calculation was repeated for the two polymer interaction and with a Li atom nearby to recognize the kind of interaction involved and the modifications in their electronic structures. Both the approaches were focused to obtain the stable structures of monomer and polymer and their possible partial array formations to know the mechanism of crystallization apart from the HOMO–LUMO gap and the corresponding electrostatic potential with charges involved for different configurations and doping.

RESULTS AND DISCUSSION

Figure 1 shows the typical cyclic voltammogram profiles and the chronopotentiometric response of the PMeT films grown on TO-coated glass substrates. From the Figure 1(a), it is clear that homogeneous deposition takes place above 1.2 V. The E–t response for a typical PMeT film deposited for 15 min at 1.52 V with a constant current density of 2.1 mA/cm^2 is shown in Figure 1(b). We can observe that after initial increase in the current (for first few seconds) it became stable through out the deposition for about 15 min, with a stable potential of about 1.52 V and a constant current density of 2.1 mA/cm^2.

Films deposited with lithium perchlorate as dopant solution were inhomogeneous. However, the films prepared with lithium terafluoroborate as dopant solution were found to be homogeneous. Therefore, for the further studies, lithium terafluoroborate solution was chosen as the dopant to dope BF_4^- anion. The amount of polymer deposited on the TO glass electrode surface increased with the increase of current density. However, for the very high current densities, the oligomeric species fall down from the surface to the solution. Though the polymer films could be deposited for the doping concentration in between 0.01 and 0.2 M, the films with higher thicknesses could be prepared only with doping solution concentration of 0.1 M. The films prepared with 0.1 M concentration solution, were of 600 nm thickness and with average conductivity about 700 S/cm. The hot probe technique revealed the films were of n-type conductivity. The electropolymerized PMeT films were of dark brown in color.

In the Figure 2(a), a typical SEM image of the films in backscattered mode is shown. The micrograph revealed the domain structures of about 3 μm size on the surface. AFM images of such domains revealed grains in the order of nanometers [Fig. 2(b)]. A further magnified AFM image (Fig. 3) revealed the aggregation of smaller grains of about 90 nm with less than 60 nm

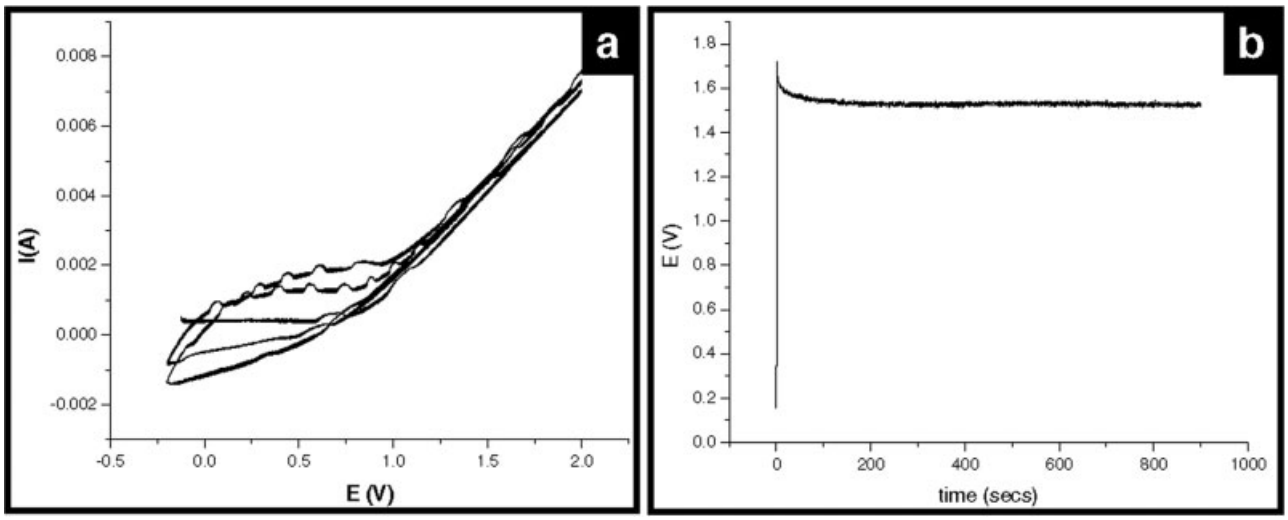

Figure 1. (a) Cyclic voltammogram profiles and (b) chronopotentiometric response monitored for the PMeT film on TO-coated glass substrate.

irregularities in height. In Figure 3, the AFM images show the 3D structure of the interior of the domains with grains of 60–125 nm in size. Also, the sectional analysis revealed the variation in the height less than 60 nm as indicated by the two different lines marked in the 2D image.

Figure 4 shows the XRD spectrum of the doped PMeT film grown on conducting glass substrate. We can observe the appearance of one well-resolved diffraction band at about $2\theta = 18.5^\circ$ and a week band at about $2\theta = 37.5^\circ$, with interplaner distances 0.467 and 0.237 nm, respectively. The appearance of such well-defined XRD bands indicates the organized structure of the polymer similar to the crystalline structure of inorganic solids. As the incorporation of dopants in PMeT forms highly confined conjugational defects, neither dynamically nor electronically coupled with the host lattice,[13] we do not expect any band related to the Li or BF_4^- dopants in the XRD pattern unless otherwise the doping concentration is

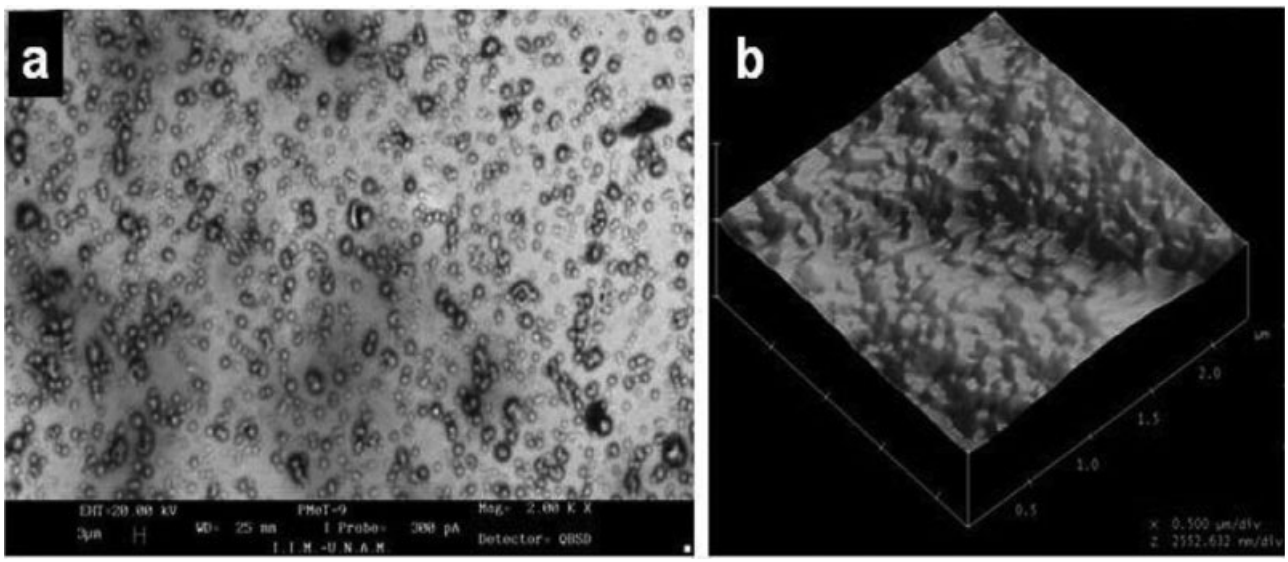

Figure 2. Surface of the sample observed by (a) backscattered electron and (b) AFM. The domains observed in the BSE signal are related more with density than superficial contrast.

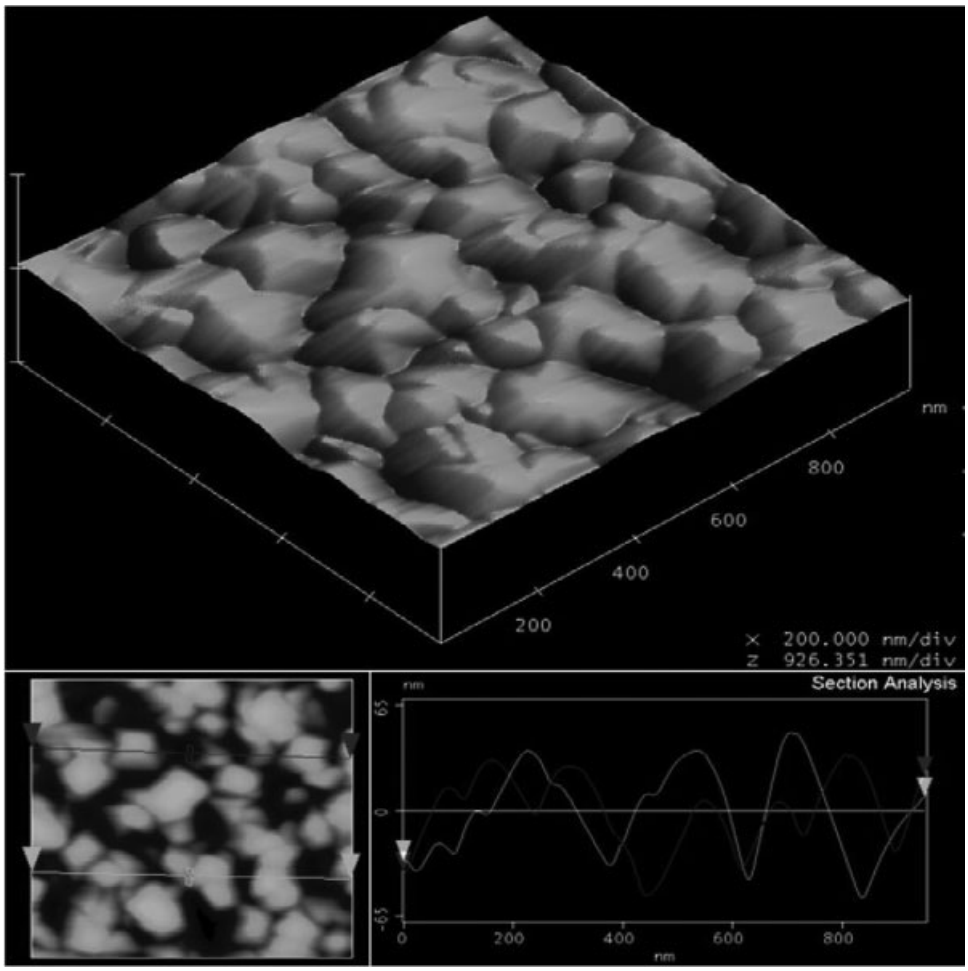

Figure 3. AFM analysis for the PMeT film surface in a 3D representation where the small domains distribution is shown; and a sectional analysis, from the two lines marked in the 2D image showing maximum height of 60 nm.

high. So far there are analyses available on the PMeT films with various dopants like ClO_4^-, BF_4^-, PF_6^- *etc.*,[3–5] but there are no reports available considering the presence of the Li ions in the polymer matrix. During the electropolymerization of the films, there is every possibility of intercalation of Li^+ trapping, even though according to Donan equilibria the possibility of Li doping is less. Hence, we assumed that the incorporated Li atoms remain intercalated in the polymer matrix and have executed the following theoretical calculations.

By means of a DFT quantum mechanical method, the optimized 2-rings structures are calculated for both cis and trans configurations. The influence of the configuration on the charge, HOMO, LUMO, electrostatic potential distributions, and Fuckui function, which denote the electrophilic $f(-)$, nucleophilic $f(+)$, and radical

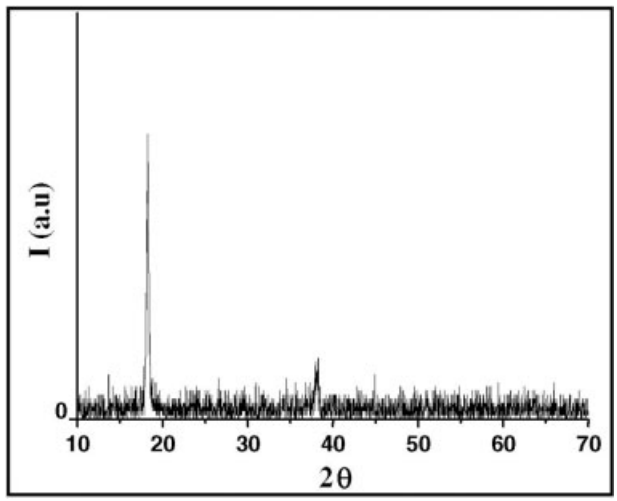

Figure 4. XRD pattern revealing partial array structure of the polymer.

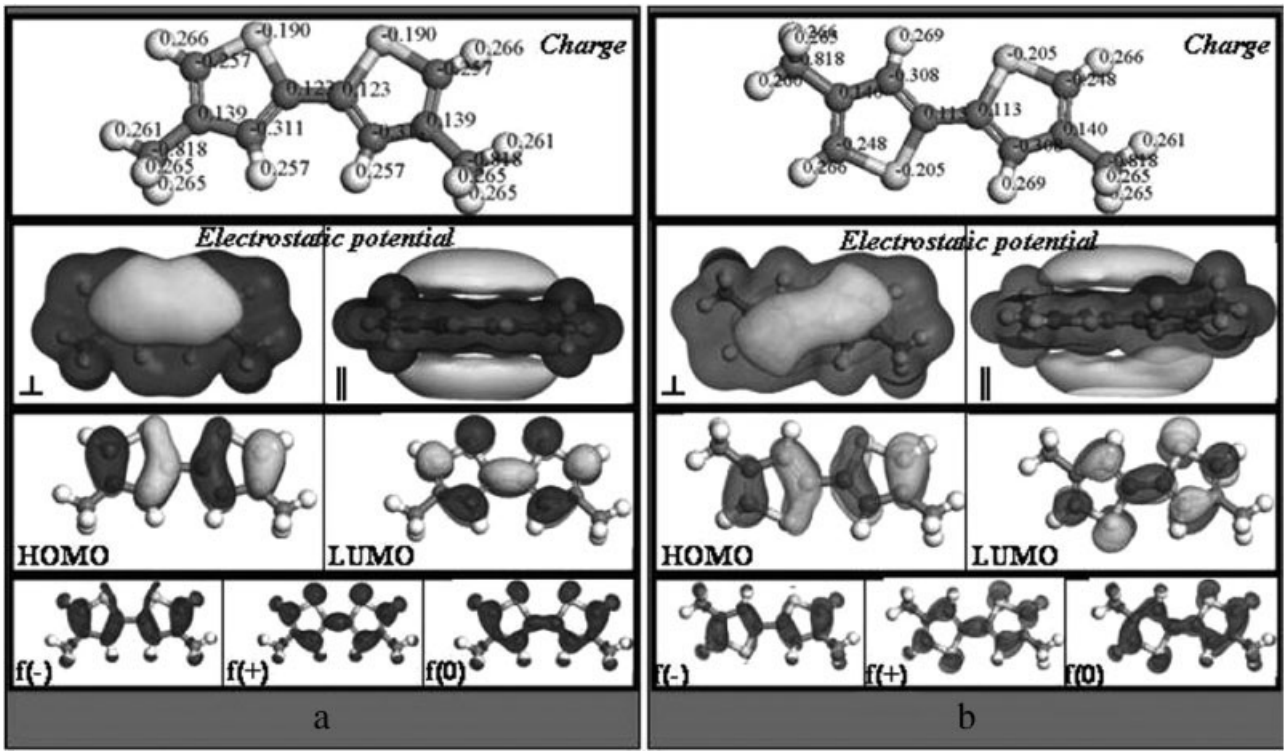

Figure 5. Polymer models for (a) cis and (b) trans configurations. For both the cases, the charge, electrostatic potential, frontier orbital distributions, and Fuckui functions are evaluated and shown.

$f(0)$ sites, are evaluated for the undoped and doped polymer.

Figure 5 shows various analyses corresponding to the cis and trans configurations of the polymer, their atomic charge, electrostatic potential, frontier orbital distributions, and Fuckui functions. In the case of cis configuration [Fig. 5(a)], the calculated charges are used to identify the most negative sites of the polymer in the carbon atoms of the rings where hydrogen is attached, while the C atoms bonded to CH_3 become the relative positive sites. In fact, there are no exposed positive sites in the structure as it was expected. The electrostatic potential is directly related to the charges, however it also allows to recognize the global zones of polarization, which is clear in the isosurfaces of both perpendicular ($\perp$) and parallel ($\|$) orientations, where the

Table 1. HOMO, LUMO, and Band Gap Values for the Different Pure and Doped Polymers, Including the Values for Extra Li Dopants and a Possible Li Cluster in Comparison With the Li Crystal

Model	HOMO (eV)	LUMO (eV)	LUMO–HOMO Gap (eV)
Cis	−4.929659	−2.212925	2.716734
Trans	−4.803619	−2.139374	2.664245
Cis+Li	−4.787102	−2.639346	2.147756
Trans+Li	−4.819374	−2.645904	2.173470
Cis–trans+Li	−4.730421	−2.703591	2.026830
Cis+2Li	−2.906993	−2.206639	0.700354
Lithium 6	−2.778421	−2.097088	0.681333
Lithium crystal	−9.138829	−0.286693	8.852136

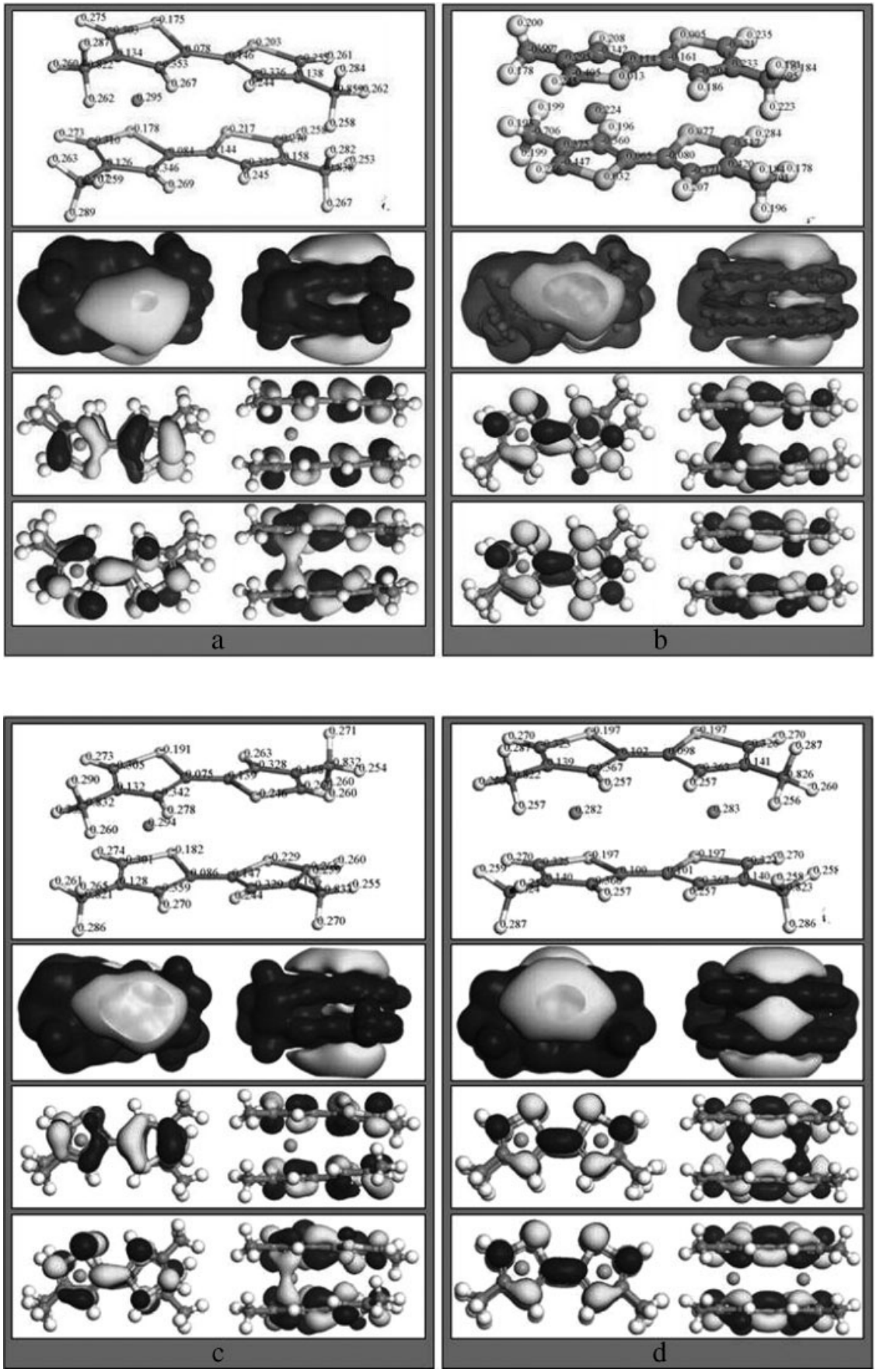

Figure 6. Quantum mechanical analysis for two molecules with a Li atom in (a) cis, (b) trans, (c) cis–trans configuration, and (d) two cis molecules with two Li atoms. In the figures, the charge, electrostatic potential, HOMO, and LUMO plots are shown for clarity.

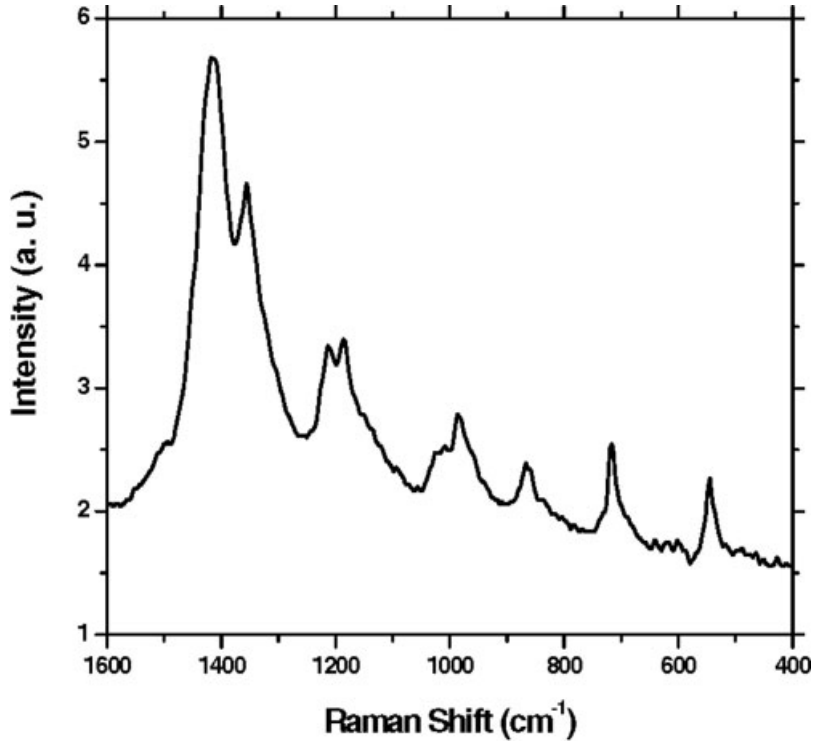

Figure 7. Raman spectrum ($\lambda_{exc} = 632.8$ nm) of doped PMeT sample.

polarization is shown by the lighter clouds dominated by the two S atoms. The frontier orbital distributions cover the entire molecule without CH_3 regions, even when the configurations are different for HOMO and LUMO. The molecular orbital and electrostatic potential distributions are common in the both cases, revealing no preferential sites to coordinate with the Li atoms, which must be placed in between the electron clouds of the rings. With the help of the Fuckui functions, we can identify in a better way the possible interaction sites for the polymer. Considering the charge of Li atom, we can predict an interaction with the electrophilic zones denoted by $f(-)$. The electrophilic zones mark the areas where the polymer has a preference to attach donor systems. So, the Li atoms must avoid the S sites and the interaction must tend to align similar zones of the polymer, causing an increase of the distance and torsion of the chains. Figure 5(b), corresponds to the trans configuration, where many similar conditions can be observed to the cis one, but there are two main differences basically in the polarization of the molecule and in the homogeneity of the isosurfaces, which is fully clear when the electrostatic potential is observed. In fact, the atomic charge also shows an interesting behavior because of the configuration, making a mirror-like effect that is easily distinguished in the figure.

Even when the differences between the structures looks small, these variations imply important changes in the electronic structure repercussions, which are evaluated in the Table 1. In Table 1, the HOMO, LUMO, and the corresponding band gap (E_g) produced between them are shown for the cis, trans, pure, and doped structures. The gaps for pure Li crystal and a possible cluster (Li 6) have also been evaluated. The values of the gap are higher for the pure polymer. However, for the doped polymer, a small difference can be observed between the structures cis (2.147 eV) and trans (2.173 eV) configurations. The band gap value is reduced (2.026 eV) when a combination of both the configurations is considered. So we can recognize an important parameter for the production of materials with a specific function from the same composition.

High Li concentration (double doping calculi) and cluster formation cases would produce much smaller gaps (Table 1) of about 0.700 and 0.681 eV,

Table 2. Proposed Assignment for the Raman Vibrational Spectrum of PMeT Doped with 0.1 M Lithium Tetrafluoroborate

Frequency (cm^{-1})	Intensity	Assignment
1414.73	vs	$\nu(C{=}C)_{ring}$
1355.07	s	$\nu(C{-}C)_{ring}$
1213.13	m	$\delta(CH)$
1185.99	m	$\nu(C{=}C)_{ring}$
1025.69	w	–
1007.18	w	$r(CH_3)$
986.16	m	δ_{ring}
863.14	m	$\nu(C{-}S)$
716.72	m	$\nu(C{-}S)$
544.83	m	$\nu(C{-}X)$

vs, very strong; s, strong; m, medium; and w, weak.

respectively, which differ significantly from the Li crystal that have an estimated value of 8.852 eV, revealing its insulating nature. Since the band gap is sensible to the minimum energy configurations, nature of dopant, dopant concentration, and coordination or accommodation of dopants in the polymer, the different band gap values for PMeT prepared by different synthesis methods allow characterizing structure of the polymer and explaining the reason for the different reported E_g values in literatures.

To understand the variation of band gap values due to the variation of electronic structure, corresponding minimum energy configurations are shown (Fig. 6) for cis and trans molecules with different Li atoms incorporated. The corresponding calculated charge, the isosurface of the electrostatic potential, and the frontier orbital distributions are presented for the different models. It is clear that in all the cases the Li atom(s) tends to be in the middle of the rings and produces a mirror-like symmetry for the molecules in the different configurations with a relative charge of 0.295, 0.224, 0.294, and two atoms with 0.282 and 0.283, respectively. While a polarized charge distribution occurred/is observed for the cis configuration, a relatively neutral charge distribution is observed when the configuration is trans.

The electrostatic isosurface potential shows that when the molecules are in cis configuration, it tends to be polarized to the zones where the S atoms are together. When the molecules are in trans configuration, the electrostatic potential distribution is more homogeneous with well-defined central zones. The molecular orbital distributions tend to be around the rings and the Li atoms generate bridges between the molecules. However, the observed distribution is clearly different for the cis and trans configurations. This behavior denotes a direct effect of the Li atoms on the redistribution of the donor and acceptor regions but also about the conditions to keep electrons in a frontier molecular orbital. The bridge is observed for the LUMO for two cis molecules [Fig. 6(a)] and cis–trans molecules [Fig. 6(c)], while the bridge is observed for the HOMO when the two molecules are trans [Fig. 6(b)] or when there are two Li atoms [Fig. 6(d)].

In Figure 7, the Raman spectrum of the PMeT film grown on SS substrate is shown. The possible assignment of Raman peaks are given in Table 2. The observed Raman peaks agree well with the experimental observation presented by Hernandez et al.[14] for the PMeT in the insulating form. We could not detect any signal related to Li or BF_4^- doping.

In Figure 8, the FTIR spectrum of the doped PMeT film grown on stainless steel substrate is shown. We could detect several IR absorption bands with different intensities in the 1420–720 cm^{-1} spectral range. The probable identification of all the bands with their relative intensities is given in Table 3.

The optical transmittance (T) spectra of the samples grown on TO-coated glass substrates were recorded from 400 to 2500 nm wavelength at room temperature using an uncoated substrate

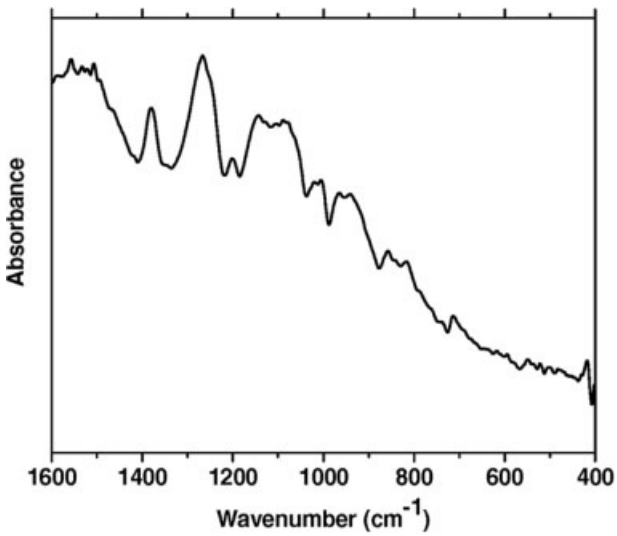

Figure 8. FTIR spectrum of PMeT doped with lithium tetrafluoroborate measured in diffused mode.

Table 3. Proposed Assignment for the IR Vibrational Spectrum of PMeT Doped with Lithium Tetrafluroborate

Frequency (cm^{-1})	Intensity	Assignment
1410	vs	$\nu(C{=}C)_{ring}$
1358	s	$\nu(C{-}C)_{ring}$
1340	vs	$\delta(CH_3)$
1220	s	$\delta(CH)$
1183	s	$\delta(CH)$
1134	w	
1040	s	$\delta(CH)$
1018	w	$r(CH_3)$
984	s	δ_{ring}
957	w	r_{ring}
878	s	$\nu(C{-}S)$
830	w	$\nu(C{-}S)$
724	w	δ_{ring}

vs, very strong; s, strong; m, medium; w, weak; vw, very weak; b, broad; and sh, shoulder.

in the reference beam. The absorption coefficient α at different wavelengths was calculated using the relation[15]

$$\alpha = 2.303 \log(1/T)\frac{1}{t}$$

where α is the absorption coefficient and t is the thickness of the films. In general, all the films showed fairly good transparency above 800 nm. The absorption coefficient of the films is related to the photon energy ($h\nu$) through the relations[16,17]

$$\alpha h\nu = A_1\left(h\nu - E_g^{d}\right)^{1/2}$$
$$\alpha h\nu = A_2\left(h\nu - E_g^{i}\right)^{2}$$

for allowed direct and indirect transitions, respectively.

Where A_1 and A_2 are two constants, E_g^{d} and E_g^{i} are the direct and indirect band gaps, respectively. A plot (Fig. 9) of $(\alpha h\nu)^{1/2}$ *vs.* $(h\nu)$ fitted well with a straight line with intercept in the energy axis at about 2.0 eV, indicating a direct nature of optical transition in the PMeT films with band gap of about 2.0 eV. This experimentally obtained E_g value coincides well with the calculated E_g value obtained for cis–trans+Li configuration presented in Table 1.

Therefore, the incorporated Li in PMeT remained in-between the polymer molecules as confined conjugational defects, neither dynamically nor electronically coupled with the host lattice. In Figure 6, the calculated LUMO of a pair of

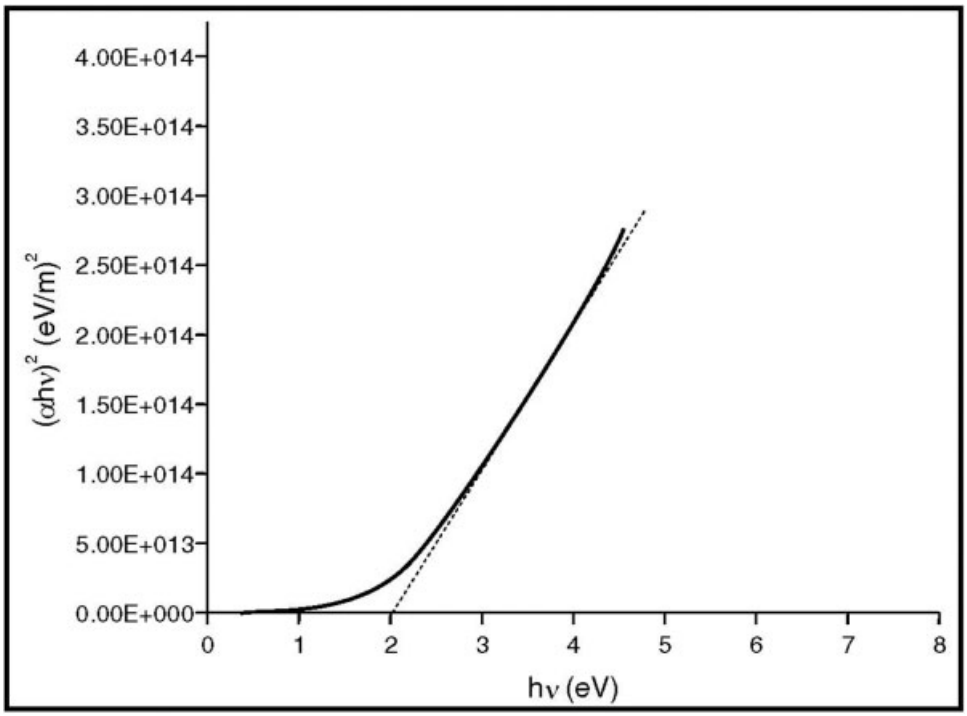

Figure 9. $(\alpha h\gamma)^2$ *vs.* $(h\gamma)$ plot for a doped PMeT film electropolymerized on conducting glass.

monomers along with a Li atom is presented, where we can observe the Li atom in between polymer structures without occupying any lattice site or substituting any atom in the main structure. The weak electronic coupling of Li with the host lattice is clear from the minimum deformation of original configuration.

CONCLUSIONS

Thin films of PMeT were prepared successfully by electropolymerization on conducting glass and stainless steel substrates. Galvanostatic method rather than potentiostatic turned out to be more effective for the preparation of PMeT films of adequate thickness on conducting glass or flexible metal surface with good adherence and homogeneity. Of lithium tetrafluoroborate and lithium perchlorate, the former was found to be a very successful in doping anions during the electropolymerization of PMeT with high conductivity (about 700 S/m). It is found that the film thickness, its adherence with conducting surface, and conductivity strongly depend on the current density, applied potential, and dopant solution concentration, respectively. The optimized potential, current density, and dopant concentration for obtaining thick, homogeneous PMeT films were 1.52 V, 2.10 mA/cm^2, and 0.1 M, respectively. The polymer thin films formed on the conducting surfaces with partially ordered structure. Absence of any signal related to lithium tetrafluoroborate in XRD, Raman, or IR spectra confirms that the incorporated dopant forms highly confined conjugational defects, neither dynamically nor electronically coupled with the host lattice. Our theoretical calculations reveled that the peaks in the XRD spectrum appear because of the partial ordering of the polymer chains and the band gap of the doped polymer depends sensibly on the geometrical configuration of the polymer and dopant concentration as well as on the polymer and Li configuration. The undoped polymer has a band gap of 2.664–2.716 eV depending on its structural configuration. Assuming the intercalation process of Li atoms in the polymer matrix, our theoretical calculation predicted a band gap of 2.026 eV for the cis and trans combination. The experimental values of the optical band gap of PMeT film were found to be about 2.00 eV, which is in well agreement with the theoretical calculations. Theoretically, the band gap can be decreased by increasing the doping concentration. Our result opens up the possibility for preparing PMeT thin films with desired optical and electrical properties for their applications in solar cell fabrication.

The work is partially supported by CONACyT, Mexico, through the project G 38618-U. Authors thank Dr. J. A. Chavez, IIM-UNAM, for the SEM analysis of the samples. We thank Ms. Margarita Miranda Hernandez, CIE–UNAM, for her valuable support during the electropolymerization of the films.

REFERENCES AND NOTES

1. Horowitz, G.; Garnier, F. Sol Energy Mater 1986, 13, 47–55.
2. Frank, A. J.; Glenis, S.; Nelson, A. J. J Phys Chem 1989, 93, 3818–3825.
3. Nguyen-Cong, H.; Sene, C.; Chartier, P. Sol Energy Mater Sol Cells 1993, 29, 209–219.
4. Chartier, P.; Nguyen-Cong, H.; Sene, C. Sol Energy Mater Sol Cells 1998, 52, 413–421.
5. Nguyen-Cong, H.; Dieng, M.; Sen, C.; Chartier, P. Sol Energy Mater Sol Cells 2000, 63, 23–35.
6. Ferro-Flores, G.; Ramírez, F. M.; Tendilla, J. I.; Pimentel-González, G.; Murphy, C. A.; Meléndez-Alafort, L.; Ascencio, J. A.; Croft, B. Y. Bioconjugate Chem 1999, 10, 726–734.
7. Ramírez, F. D.; Sosa-Torres, M. E.; Escudero, R.; Padilla, J.; Ascencio, J. A. J Coord Chem 2000, 50, 1–16.
8. Ascencio, J. A.; Rodrguez-Lugo, V.; Angeles, C.; Santamaria, T.; Castano, V. M. Comp Mat Sci 2002, 25, 413–426.
9. Sun, Z. W.; Frank, A. J. J Chem Phys 1991, 94, 4600–4608.
10. Kobel, W.; Kiess, H.; Egli, M.; Keller, R. Mol Cryst Liq Cryst 1986, 137, 141–150.
11. Delley, B. J Chem Phys 1990, 92, 508–517.
12. Delley, B. J Chem Phys 2000, 113, 7756–7764.
13. Lopez-Navarrete, J. T.; Zerbi, G. J Chem Phys 1991, 94, 965–970.
14. Hernandez, V.; Ramirez, F. J.; Otero, T. F.; Lopez-Navarrete, J. T. J Chem Phys 1994, 100, 114–129.
15. Velumani, S.; Mathew, X.; Sebastian, P. J.; Narayandass, S. K.; Mangalaraj, D. Sol Energy Mater Sol Cells 2003, 76, 347–358.
16. Pal, U.; Saha, S.; Chaudhuri, A. K.; Rao, V. V.; Banerjee, H. D. J Phys D: Appl Phys 1989, 22, 965–970.
17. Tauc, J. In Optical Properties of Solids; Abeles, F., Ed.; North-Holland: Amsterdam, 1972.